Analytical and Numerical Methods in Mechanical Design
Vol.1, Issue 1, Winter & Spring 2022, 19 - 29

Fracture Analysis of Conical Shells Containing an Internal Semi-Elliptical Crack

C. Burvill [1], M.M. Kheirikhah[1,*] , S. Omidi[2], S. Gohari[1]

[1] *Department of Mechanical Engineering, the University of Melbourne, Parkville, VIC 3010, Australia.*
[2] *Faculty of Industrial and Mechanical Engineering, Qazvin Branch, Islamic Azad University, Qazvin, Iran.*
Received: 08 February 2022- Accepted: 11 April 2022
*Corresponding author : *kheirikhah@qiau.ac.ir*

Abstract

Conical shells play a significant role in different branches of engineering such as aerospace and oil industries. The purpose of this paper is to analyze the fracture behavior of metallic conical shells containing an internal semi-elliptical crack. An accurate three-dimensional finite element method is employed to model the conical shell using ANSYS standard code. Special singular elements are used to consider the square-root singularity at the semi-elliptical crack front. Stress intensity factors of the cracks which placed in different positions of the shell is calculated. To confirm the accuracy of the present finite element model, both stress distribution of the structure and stress intensity factor of the crack in special case are compared with published results. The effect of different geometrical parameters on the stress intensity factor of the cracks are investigated. Results show that the crack aspect ratio has a significant effect on the stress intensity factor of the cracks.

***Keywords*:** Fracture Analysis, Stress Intensity Factor, Conical Shell, Finite Element Method, Semi-Elliptical Crack.

1. Introduction

Conical structures play important role in engineering applications such as nozzles, engines, rockets and power plant equipment [1,2]. During service time, these structures are subjected to thermo-mechanical loads and corrosion conditions which cause to appear cracks and surface defects on their materials. These cracks are the main cause of fracture and failure in these structures which increase costs of repair and maintenance. Scientific researches show that crack initiation with an arbitrary shape in shells transform to semi-elliptical shape when the structure is subjected to dynamic loading [3]. Semi-elliptical surface cracks are generally found in the industrial process and in the products service life. These cracks are one of the most important factors which cause to shell structures become fail. Therefore, fracture analysis of cylindrical and conical shells with semi-elliptical cracks in their walls is a hot subject in this field. To predict the mechanical behaviors and fracture of the cracked shell structures, the stress intensity factor (SIF) is the most important parameter. Generally, the linear elastic fracture mechanics is applied to calculate the SIFs along the crack front. Also, to evaluate the crack growth rates and fracture strength of these structures, many investigators have used engineering estimation or numerical analysis to obtain the SIFs.

To date, there are many papers have been published on fracture analysis of cylindrical shell structures. In leading efforts, the wall thickness effect on the fracture analysis of cylinders and pipes was ignored [4,5]. Through a line-spring model, Delale and Erdogan [6] reached relatively solution for cylindrical shell including an axial or circumferential semi-elliptical surface crack. Raju and Newman [7] used the finite element method (FEM) to compute the SIF of a cracked cylinder for different crack sizes. The cylinder has been subjected to various stress distributions. Wang and Lambert [8] presented the SIF for longitudinal semi-elliptical cracks in pipes using weight function method. Lin and Smith [3] estimated crack growth behavior for cracked cylindrical pressure vessels under dynamic loadings.

Bergman [9] used the FEM to estimate the J-integral for part circumferential surface cracks in pipes. He showed that there is no significant difference between outside and inside surface cracks. Carpinteri [10] studied fracture analysis of semi-elliptical cracks in round bars subjected to axial tension. He found that the maximum of the mode I SIF is happened at the deepest point of semielliptical cracks for flaw aspect ratios. Shin and Cai [11] investigated the shafts under axial and flexural loadings with an elliptical surface crack, experimentally and numerically. Diamantoudis and Labeas [1] used an advanced FEM to calculate the SIF of semi-elliptical cracks located in the critical portion of a pressure vessel for various geometrical parameters.

Moreover, fatigue crack growth of axial surface cracks in cylindrical pressure vessels was investigated by Shahani and Habibi [12] using 3-dimensional (3D) FE analysis. They studied the analysis for different geometric parameters and assumed material plasticity and combination loadings. Fracture analysis of composite hoop-wrapped steel-lined

compressed natural gas (CNG) cylinders was also presented by Shahani and Kheirikhah [13]. Nabavi and Shahani [14] studied fracture analysis of thick-walled cylinders containing internal semi-elliptical cracks under thermo-mechanical loads. El Hakimi et al. [15] presented the SIF and J integral for internal and external semi-elliptical cracks of cylindrical and spherical shells using the FEM. The T-stress solutions for semi-elliptical axial cracks in a cylinder subjected to uniform, linear and parabolic stress distributions were presented by Meshii et al. [16]. Wen et al. [17] analyzed the creep fracture behavior of a metallic cylinder with a semi-elliptical internal crack subjected to thermo-mechanical loadings using the FEM.

In addition, Predan et al. [18] calculated mode II, mode III and mixed mode SIFs for semi-elliptical cracks in a hollow cylinder. They used the FEM and the cylinder was subjected to torsion. Based on 3D FEM, Yang et al. [19] proposed a weight function method to calculate the SIFs for semi-elliptical cracks in cylindrical pressure vessels. They found that at the surface point, the cracks with higher aspect ratios have the larger SIF. Okada et al. [20] expanded a parametric analysis procedure to calculate the SIF for the cracked thick-wall flat plates. They found that the SIF solutions for the thick wall cylinder could be estimated by those for the flat plate. Zareei and Nabavi [21] measured the SIF at the deepest point of a high aspect ratio semi-elliptical circumferential crack in a pipe. Shariati et al. [22] proposed the fatigue testing specimen to predict the path and the rate of crack growth in thick-walled pressure cylinders with semi-elliptical cracks. Effect of the arc welding process and mechanical loading on the SIF of cracked thin Aluminum cylinders was simulated by Aliha and Gharehbaghi [23] using the 3D FEM. Based on a weight function method, Alizadeh Kaklar and Saeidi Googarchin [24] provided SIFs for all points on the front of semi-circular cracks in an arbitrary structure under various two-dimensional stress distributions. Ramezani et al. [25] presented empirical solutions for all modes SIFs of a semi-elliptical crack in the surface of a bar subjected to torsion. Effect of temperature on the fatigue crack growth of external semi-elliptical surface cracks in aluminum alloy hollow cylindrical specimens under constant load amplitude was experimentally investigated by Shlyannikov et al. [26].

Moreover, during last two decades, fracture analysis of semi-elliptical crack in advanced materials has been considered by scientists and researchers. Kheirikhah and Khalili [27] studied fracture analysis of semi-elliptical cracks at the interface of two functionally graded materials (FGM). They investigated the impact of discontinuity of the mechanical properties on the SIF of semielliptical cracks. The SIF of a semi-elliptical circumferential surface crack placed on the wall-thickness of a FGM cylinder were presented by Nami and Eskandari [28]. The SIF of internal surface cracks was calculated in auto-frettaged FG cylinders using weight function method by Seifi [29]. Farahpour et al. [30] presented the SIF for semi-elliptical cracks on cylinders with a metallic liner and FGM coating. The effects of the cylinder geometry, composite layer thickness, and the property distributions of the composite layers on the SIFs of hoop-wrapped CNG cylinders were investigated by Chen and Pan [31]. Eskandari [32, 33] studied fracture analysis of FGM-coated cylinders and tubes containing semielliptical internal crack subjected to temperature loading using FEM. The SIF of semielliptical cracks at the Reactor pressure vessel nozzle–cylinder intersection was presented by Murtaz and Hyder [34] using elastic and elasto-plastic FEM. Fiber reinforced composites pipelines with axial and circumferential semi-elliptical cracks were investigated by Wang et al. [35] using the FEM. Mode I delamination failure behavior of filament-winded composite pipes was studied experimentally and numerically by Rekbi et al. [36].

Mechanical behavior of conical shells subjected to thermos-mechanical loadings has been also studied by some researchers [37]. But, it seems, there are no published articles about fracture analysis of conical shells. Therefore, in this paper, fracture analysis of conical shells is presented. The semi-elliptical surface crack into the conical shell wall is simulated via 3D FEM. The SIF of the cracks is calculated for different crack geometries such as shell thickness, cone height, and crack aspect ratio.

2. Finite Element Modeling

In this paper, metallic thin-wall conical shells with semi-elliptical axial surface cracks are investigated. The cross section and geometrical parameters of the cracked shell are shown in Fig. 1. Because of symmetry, only a half of the conical shell is modeled. In this Fig., H is the shell height, T is the wall thickness and R1 and R2 are the upper and lower radius of the shell, respectively. The semi-elliptical crack is placed in the center or corner of the shell.

Because the longitudinal surface cracks are more critical than the circumferential ones [19], an internal longitudinal semi-elliptical crack with length of 2c and depth of a is supposed. Semielliptical cracks are often described with two dimensionless parameters: the aspect ratio (a/c) and the relative depth (a/t) [13]. As shown in Fig. 1, the points A and C are called the surface points and the point B is named as the deepest point [14].

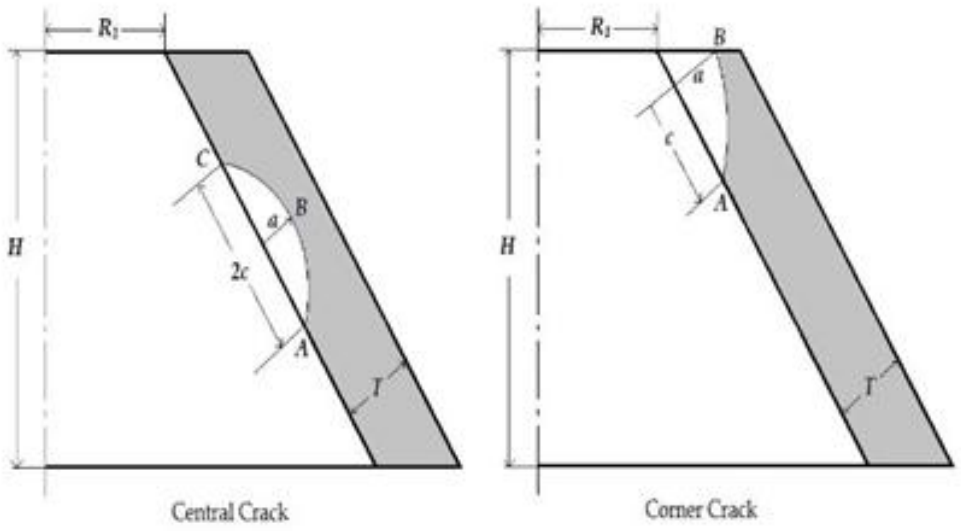

Fig. 1. Typical cross-section of the conical shell with an internal semi-elliptical longitudinal central or corner crack.

The aluminum material is used for modeling of the shell which its properties are defined as following:

$$E = 70 \text{ GPa} \quad \text{and} \quad v = 0.3 \tag{1}$$

where E is the Young moduli and v is the Poisson's ratio.

In this section, the FE modelling of the conical shell contains a semi-elliptical crack in the center of the shell is explaining. The model is constructed using ANSYS 17.0 commercial code. Due to the symmetry in the geometry and loading of the problem, only a half of the conical structure is modelled. Hence, only one of the two elliptical crack surfaces is also built.

To accurate modelling of the crack, the crack-tip stress square-root singularity must be modelled. The first devised method for Quarter point elements was presented by Barsoum [38]. In this method, the mid-side nodes of isoparametric elements, which are located around the crack-tip, are shifted to the quarter point locations. Hence, this approach is applied in the present work to model the crack-tip stress singularity.

To make the model, first the crack front tunnel is constructed by extruding a temporary plane along the semi-elliptical crack front using 20-nodes brick elements [13]. Fig. 2 shows the meshed crack tunnel. Then, the crack plane shown in Fig. 2 is also meshed by 2D elements. Finally, the complete FE model of the problem can be constructed by sweeping the crack plane around the central axis of the cone using 20-nodes brick elements. Fig. 3 shows the complete 3D FE model of the conical shell with an internal semi-elliptical longitudinal crack at its center. In this Figure, the XZ plane is the symmetry plane of the problem. Such procedure can be applied to construct the FE model of the shell contains a semi-elliptical crack in the corner of the shell.

Because the problem has geometrical and physical symmetry and the XZ plane is the symmetrical plane, only a half of the shell is modeled. Thus the normal displacement component of this plane must be constrained. On the other hand, for solving this problem needs to be constrained the displacement of the top edge of the shell along the longitudinal direction (X-direction). Since the boundary conditions of the problem can be defined as:

$$\begin{aligned} &\text{For XZ plane:} && w\,(y = 0) = 0 \\ &\text{For top edge of the shell:} && u\,(x = 0) = 0 \end{aligned} \tag{2}$$

where u and w are the displacements along the X and Z directions, respectively. A constant internal pressure is applied to the all inner surfaces of the shell. Because the crack is considered internally, the pressure is also applied to the crack surface. Finally, the SIFs of the crack's front points is computed by ANSYS 17.0 standard code.

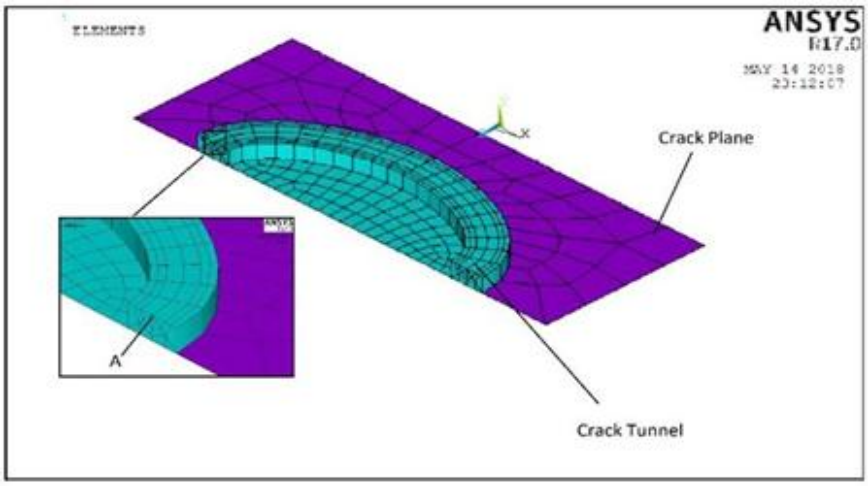

Fig. 2. Constructing the crack tunnel using 3D singular elements

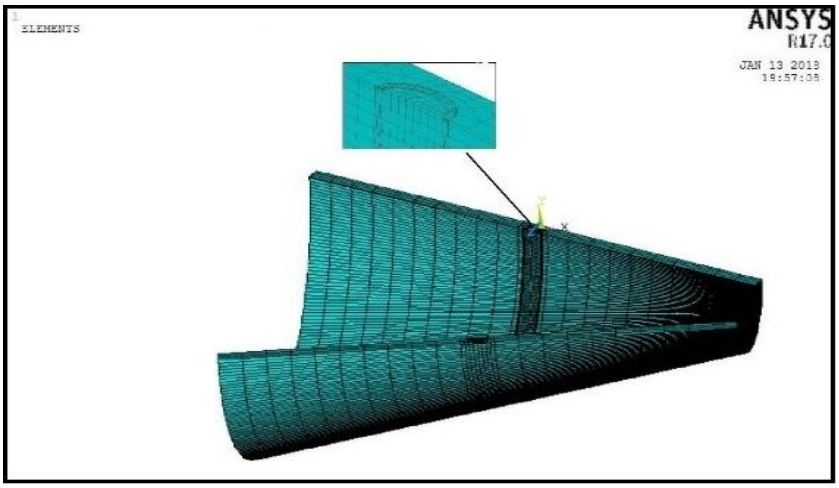

Fig. 3. Complete 3D FE model of the conical shell with an internal semi-elliptical longitudinal crack.

3. Results and Discussion

The validity of the FE modeling and analysis is examined in this section. To determine the accuracy of the present FE modeling and before the Stress Intensity Factor (SIF) calculation, the stress distribution along the wall of a crack-free conical shell is calculated by the present 3D FE modeling and compared with those of reported results by Ugural [37]. Fig. 4 shows the typical geometrical parameters of the constructed crack-free conical shell. A constant concentrated circular edge force $P_C = 339.5\ N/m$ is applied to the top edge of the shell.

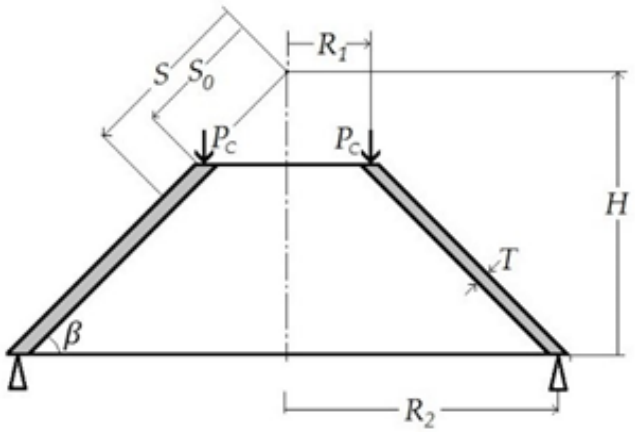

Fig. 4. Schematic of the conical shell.

Based on the analytical solutions [37], the membrane stresses in the shell can be calculated as:

$$\sigma_S = -P_C \frac{S_0}{S.T} \frac{1}{Sin\ \beta} \tag{3}$$

where σs is the membrane stresses, β is the cone base angle, S is the distance measured along generator from conical shell apex and T is the wall thickness. In this example, the thickness is assumed T = 0.001 m and also S and S_0 are supposed 0.3125 m and 0.125 m, respectively. It should be noted that the shear stress and tangential normal stress are vanished (σ_θ = $\tau_{s\theta}$ = 0). Table 1 presents the calculated membrane stress of the conical shell. It can be seen that the present results are in excellent agreement with the exact solution.

As discussed, based on authors' knowledge, no published articles have been presented for the fracture analysis of semielliptical cracks on the inner surface of conical shells. But, the SIF for semi-elliptical cracks on the wall of cylinder shells was presented by Raju and Newman [7]. In special case (β = 90), the conical shell can be transformed to cylindrical shell. In the present paper, to evaluate the accuracy for the present FE modeling and SIF calculation, a cylindrical shell contains a semi-elliptical internal crack is modeled and analyzed and the obtained results are compared with those published results. Base on presented paper by Raju and Newman [7], the mode I dimensionless SIF of semielliptical crack in the wall of a cylinder can be calculated as:

$$K_I^* = \frac{K_I}{\frac{PR}{t}\sqrt{\pi \frac{a}{Q}}} \tag{4}$$

Table 1. Membrane stress of the conical shell

H/R2	φ (degree)	Ugural [37] (Pa)	Present (Pa)	Error (%)
2/3	33.69	244838	244148	0.2818
3/3	45	192067	194307	1.166
4/3	53.13	169765	169984	0.129
5/3	59.03	158382	158731	0.22
6/3	63.43	151842	152021	2.8

Table 2. Mode I SIF for semi-elliptical crack in a cylinder

φ (Rad)	2 φ / π	Raju and Newman [7]	Present	Error (%)
0	0	1.32	1.274	3.5
π/16	0.125	1.27	1.255	1.2
π/8	0.25	1.21	1.248	3.2
3π/16	0.375	1.17	1.248	6.7
π/4	0.5	1.15	1.242	8.0
5π/16	0.625	1.16	1.246	7.5
6π/16	0.75	1.195	1.249	4.5
7π/16	0.875	1.217	1.241	2.0
π/2	1	1.21	1.244	2.8

where K_I is the mode I SIF of semi-elliptical crack, P is the applied internal pressure, R is the cylinder radius, t is the wall thickness of the cylinder and the Q parameter can be defined as [7]:

$$Q = 1 + 1.464 \left(\frac{a}{c}\right)^{1.65} \tag{5}$$

In this example, the internal pressure is assumed P = 1 MPa, the thickness to radius ratio is assumed $t/R = 0$ and crack aspect ratio is assumed a/c = 1. Table 2 compares the SIF for a semielliptical internal crack front in the wall of the cylinder. It can be seen that the present results are in good agreement with the published results by Raju and Newman [7] and the maximum discrepancy is 8 percent. Therefore, these two examples confirm that the present FE analysis is accurate and reliable.

The variation of the dimensionless mode I SIF (K_I/K_0) of an internal crack versus the crack depth ratio (a/t) for the surface point (A) and the deepest point (B) is shown in Fig. 5 where the K_0 can be calculated as:

$$K_0 = P\sqrt{\pi a} \tag{6}$$

In this equation, P is the applied internal pressure. Moreover, in this example, the constant geometry parameters are considered as a/c = 1, T = 0.001 m, H = 0.4 m and R_1/R_2 = 1.25. The simply supported boundary conditions are applied to the lower edge of the cone. The analysis is performed for different thickness ratios (a/t = 0.3, 0.5, 0.6, 0.7 and 0.8). The values of the SIF for both points A and B increase with increase in crack depth ratio (a/t), but the dimensionless SIF (K_I/K_0) of point A decreases with increase in a/t ratio. The dimensionless SIF is divided by K_0 and based on equation (6) the K_0 increases with increase in a/t ratio. Because the increasing rate of K_0 is more than the increasing rate of K_I of point A, therefore the dimensionless SIF of this point decreases with increase in a/t ratio. In point B, the increasing rate of K_0 is less than the increasing rate of K_I, therefore the dimensionless SIF of point B increases with increase in a/t ratio.

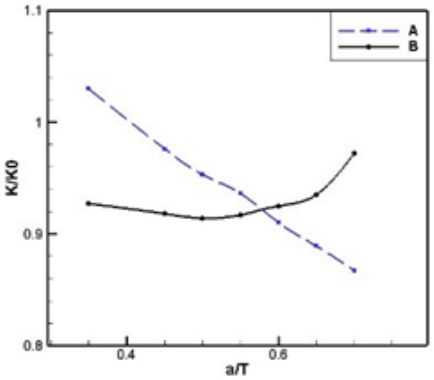

Fig. 5. Variation of the dimensionless mode I SIF against the relative depth ratio in a corner-crack.

Fig. 6 presents the variation of the dimensionless mode I SIF (K_I/K_0) of a central crack regarding the crack depth ratio (a/t) for the surface points (A, C) and the deepest point (B). The constant geometrical parameters are assumed as $R1/R2$ = 1.25, H = 0.4 m, a/c = 1, T = 0.001 m. The analyses are performed for different crack depth ratio ratios (a/T= 0.3, 0.5, 0.6, 0.7 and 0.8). The boundary conditions and K_0 are same as previous analysis. It can be seen that the SIF values for both surface points (A and C) are close together. Also, the dimensionless SIFs of all points increase with the increase in aspect ratio. Shahani and Kheirikhah [13] confirmed that the dimensionless SIF of the deepest point of cracked cylinder increases with increase in a/t ratio. It can be seen that this behavior is repeated for cracked cones.

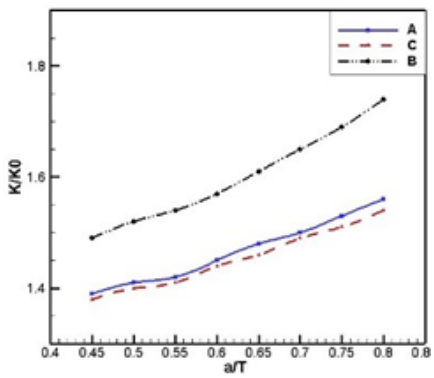

Fig. 6. Variation of the dimensionless mode I SIF against the relative depth ratio in a central crack.

Figs. 7 and 8 show variations of normalized mode I SIF (K_I/K_0) versus the height to upper radius ratio (H/R_1) for corner crack and central crack, respectively. The variation of the normalized mode I SIF (K_I/K_0) of the deepest and surface points of the central crack is shown in Fig. 7. The geometrical parameters are supposed R_1/R_2 =1.25, a/T=0.5, a/c = 1, T = 0.001 and R_1 =0.3 m. The analyses are done for different height to upper radius ratios (H/R1) varying from 0.3 to 1.3. This figure shows that variation of mode I SIF for both points has same behavior. Two lines crossed each other at *H/R1* of about 0.45. It can be seen that the SIFs for H/R_1> 0.4 are approximately constant. Fig. 8 compares the normalized mode I SIF (K_I/K_0) for the surface points A and C and the deepest point B in terms of *H/R1* (height and radius ratio) for a central crack. Besides, constant parameters are R_1/R_2 =1.25, a/T = 0.5, a/c = 1, T = 0.001 m, R_1 = 0.15 m. It can be seen that the variation of these graphs are same as graphs of the corner crack (Fig. 7). Also, this Fig. shows that the normalized mode I SIFs of the surface points are close together and the normalized mode I SIFs of deepest point are higher than those of surface points. The variation of SIF for central crack has same behavior as corner crack and the SIFs for H/R_1> 0.2 are approximately constant.

Figs. 9 and 10 show variations of normalized mode I SIF (K_I/K_0) in terms of the crack aspect ratio (a/c) for the corner crack and the central crack, respectively. The geometrical parameters are supposed R_1/R_2 =1.25, a/T=0.5, T = 0.001, H = 0.4 m and R_1 =0.3 m. The analyses are done for different crack aspect ratios. Fig. 9 shows that the curve of the surface point (A) crosses the curve of the surface point (B) at a/c = 0.9. Hence, it can be drawn that for slender corner cracks (a/c < 0.9), the surface points have smaller SIF than the deepest points, but for the deep corner cracks (a/c > 0.9), including semi-circular cracks (a/c = 1), the surface points have larger SIF than the deepest points. This aspect ratio which the curves cross each other and the location of greater SIF changes is called 'transition aspect ratio [14]. It means that the semi-elliptical cracks tend to convert to semi-circular shape. These behavior has been reported by published papers [13, 14]. In Fig. 10, it can be seen that the normalized mode I SIFs of the both surface points (A and C) and transition aspect ratio of the central crack is a/c = 1.23. Therefore, in semi-circular central cracks (a/c = 1), the normalized mode I SIFs of the deepest point is larger than the normalized mode I SIFs of the surface points.

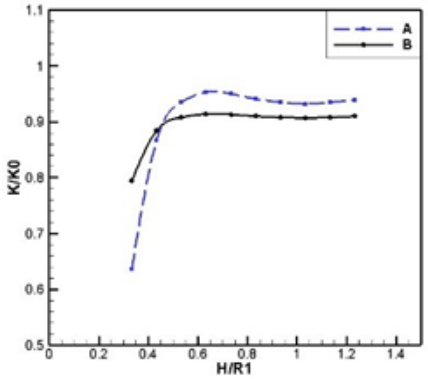

Fig. 7. Variations of mode I SIFs against the conical height to upper radius (H/R1) for corner crack

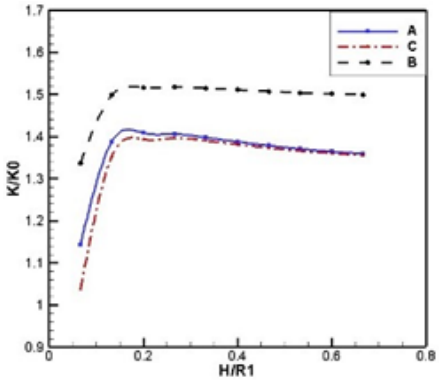

Fig. 8. Variations of the SIFs against the conical height to upper radius (H/R1) for central crack.

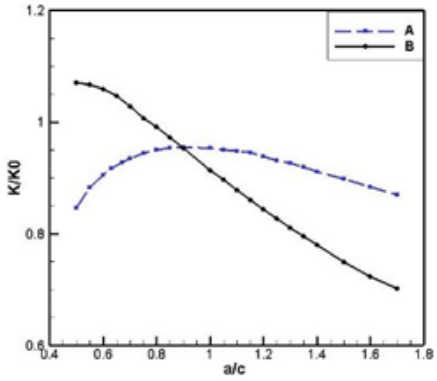

Fig. 9. Variations of the SIFs against the crack aspect ratio (corner crack)

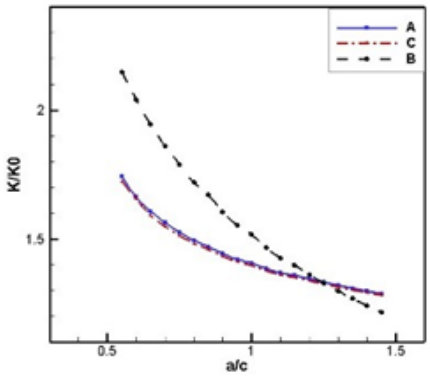

Fig. 10. Variations of the SIFs against the crack aspect ratio (central crack)

Fig. 11 shows the normalized mode I SIFs for the surface point (A) and the deepest point (B) of a corner crack versus thickness to radius ratio (*T/R1*). In this figure, the constant geometry parameters are considered as R_1/R_2 =1.25, a/T = 0.5, a/c = 1, R_1 = 0.3 m and H = 0.4 m. The analyses are performed for different thickness to radius ratios (T/R_1 = 0.001, 0.002, 0.003, 0.02). It can be drawn that the mode I SIFs of the surface point are higher than those for the deepest point. Also, it is found that increase in relative thickness-to-upper radius ratio (T/R_1) decreases the mode I SIF because increasing the thickness cause to reduce the stress distribution through the wall of the shell and the SIF.

The variation of normalized mode I SIFs for the surface points (A, C) and the deepest point (B) of a central crack versus shell thickness to radius ratio (T/R_1) are illustrated in Fig. 12. All the constant geometry parameters are same as Fig 11. Similar to corner crack (Fig 11.), the mode I SIFs of all points decrease with increase in relative thickness-to-upper radius ratio (T/R_1). But, in opposite to corner crack (Fig. 11), the mode I SIFs of the deepest point of the central crack are higher than those of the surface points. It happens because of different transition aspect ratios of the corner and central cracks. As discussed before (Figs. 9 and 10), the transition aspect ratio of corner cracks is a/c = 0.9 and for central cracks is a/c = 1.23. Therefore, for semi-circular cracks (a/c = 1), the SIFs of deepest point of corner crack is smaller than those of surface point (Fig. 11) while the SIFs of deepest point of central crack is larger than those of surface points (Fig. 12).

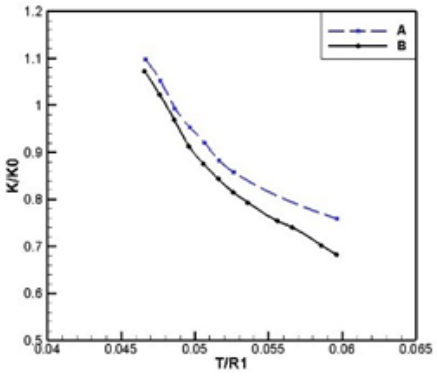

Fig. 11. Variations of the SIFs against the conical thickness (corner crack).

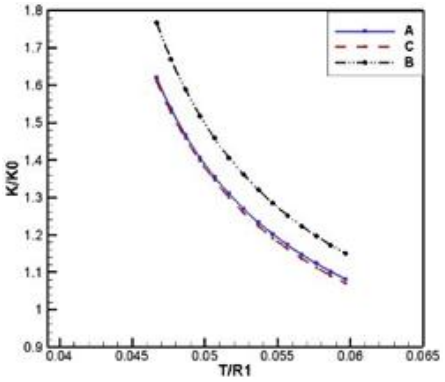

Fig. 12: Variations of the SIFs against the conical thickness (central crack)

4. Conclusions

In this paper, fracture analysis of conical shells with a semi-elliptical internal crack was studied. The 3D FEM was used for modeling and construction of the structure. Also, square-root singular elements were employed to model the crack front. The accuracy of the presented FE model was tested via two special problems. The obtained results were in good agreement with those of published results and confirmed that the present analysis is accurate and reliable.

Based on obtained results, it can be concluded the SIF of surface and deepest points increase with increase in crack depth ratio (a/t). The variation of SIF against height to top radius ratio (H/R_1) for both corner and central cracks has same behavior and for greater H/R_1 the SIFs are approximately constant. In addition, the mode I SIFs decrease with increase in relative thickness-to-upper radius ratio (T/R_1).

Moreover, results confirmed that crack aspect ratio plays a significant role in fracture behavior of conical shells. For each type of crack in a conical shell, there is a transition aspect ratio which is close to 1. For slender cracks which their aspect ratios are smaller than the transition aspect ratio, the surface points have smaller SIF than the deepest points. But, for deep cracks with larger aspect ratios than the transition aspect ratio, the deepest point have smaller SIF than the surface points. It means that the semi-elliptical cracks tend to convert to semi-circular shape.

References

[1] Diamantoudis, A. T. and Labeas, G. N. (2005) 'Stress intensity factors of semi-elliptical surface cracks in pressure vessels by global-local finite element methodology', Engineering Fracture Mechanics, 72(9), pp. 1299–1312. doi: 10.1016/j.engfracmech.2004.10.004.

[2] Moustabchir, H. et al. (2010) 'Experimental and numerical study of stress-strain state of pressurised cylindrical shells with external defects', Engineering Failure Analysis. Elsevier Ltd, 17(2), pp. 506–514. doi: 10.1016/j.engfailanal.2009.09.011.

[3] Lin, X. B. and Smith, R. a (1998) 'Fatigue Growth Prediction of Internal Surface Cracks in Pressure Vessels', Journal of Pressure Vessel Technology, 120(1), pp. 17–23. doi: 10.1115/1.2841878.

[4] Underwood, J. (1972) 'STP34113S @ www.astm.org'. In: Stress Analysis and Growth of Cracks: Proceedings of the 1971 National Symposium on Fracture Mechanics: Part 1. ASTM International; 1972. https://doi.org/10.1520/STP34113S.

[5] Emery, A. F., Love, W. J. and Kobayashi, A. S. (1976) 'Elastic Crack Propagation Along a Pressurized Pipe', Journal of Pressure Vessel Technology, 98(1), pp. 2–7. doi: 10.1115/1.3454320.

[6] Delale, F. and F. Erdogan (1984) 'Application of Line-Spring Model To a Stiffened Cylindrical Shell Containing an Axial Part-Through Crack', Fracture 84, 49(March 1982), pp. 1037–1044. doi: 10.1016/B978-1-4832-8440-8.50084-3.

[7] Raju, I. S. and Newman, J. C. (1982) 'Stress-Intensity Factors for Internal and External Surface Cracks in Cylindrical Vessels', Journal of Pressure Vessel Technology, 104(4), p. 293. doi: 10.1115/1.3264220.

[8] Wang X, Lambert SB. (1996) 'Stress intensity factors and weight functions for longitudinal semi-elliptical surface cracks in thin pipes', Int J Press Vessel Pip. 65(1):75–87. https://doi.org/10.1016/0308-0161(94)00160-K.

[9] Bergman, M. (1995) 'Stress Intensity Factors for Circumferential Surface Cracks in Pipes', Fatigue & Fracture of Engineering Materials & Structures, 18(10), pp. 1155–1172. doi: 10.1111/j.1460-2695.1995.tb00845.x.

[10] Carpinteri, A. (1993) 'Shape change of surface cracks in round bars under cyclic axial loading', International Journal of Fatigue, 15(1), pp. 21–26. doi: 10.1016/0142-1123(93)90072-X.

[11] Shin, C. S. and Cai, C. Q. (2004) 'Experimental and finite element analyses on stress intensity factors of an elliptical surface crack in a circular shaft under tension and bending', International Journal of Fracture, 129(3), pp. 239–264. doi: 10.1023/B:FRAC.0000047784.23236.7d.

[12] Shahani, A. R. and Habibi, S. E. (2007) 'Stress intensity factors in a hollow cylinder containing a circumferential semi-elliptical crack subjected to combined loading', International Journal of Fatigue, 29(1), pp. 128–140. doi: 10.1016/j.ijfatigue.2006.01.017.

[13] Shahani, A. R. and Kheirikhah, M. M. (2007) 'Stress intensity factor calculation of steel-lined hoop-wrapped cylinders with internal semi-elliptical circumferential crack', Engineering Fracture Mechanics, 74(13), pp. 2004–2013. doi: 10.1016/j.engfracmech.2006.10.014.

[14] Nabavi, S. M. and Shahani, A. R. (2009) 'Thermal stress intensity factors for a cracked cylinder under transient thermal loading', International Journal of Pressure Vessels and Piping. Elsevier Ltd, 86(2–3), pp. 153–163. doi: 10.1016/j.ijpvp.2008.11.024.

[15] El Hakimi, A., Le Grognec, P. and Hariri, S. (2008) 'Numerical and analytical study of severity of cracks in cylindrical afile:///media/saber/Saber's%20volume/P/New%20folder/2019/references nd spherical shells', Engineering Fracture Mechanics, 75(5), pp. 1027–1044. doi: 10.1016/j.engfracmech.2007.04.027.

[16] Meshii, T., Tanaka, T. and Lu, K. (2010) 'T-Stress solutions for a semi-elliptical axial surface crack in a cylinder subjected to mode-I non-uniform stress distributions', Engineering Fracture Mechanics. Elsevier Ltd, 77(13), pp. 2467–2478. doi: 10.1016/j.engfracmech.2010.06.007.

[17] Wen, J. F. et al. (2011) 'Creep fracture mechanics parameters for internal axial surface cracks in pressurized cylinders and creep crack growth analysis', International Journal of Pressure Vessels and Piping. Elsevier Ltd, 88(11–12), pp. 452–464. doi: 10.1016/j.ijpvp.2011.08.005.

[18] Predan, J., Močilnik, V. and Gubeljak, N. (2013) 'Stress intensity factors for circumferential semi-elliptical surface cracks in a hollow cylinder subjected to pure torsion', Engineering Fracture Mechanics, 105, pp. 152–168. doi: 10.1016/j.engfracmech.2013.03.033.

[19] Yang ST, Ni YL, Li CQ. (2013) 'Weight function method to determine stress intensity factor for semi-elliptical crack with high aspect ratio in cylindrical vessels', Eng Fract Mech. 109: 138–49. https://doi.org/10.1016/j.engfracmech.2013.05.014.

[20] Okada, H. et al. (2016) 'Computations of stress intensity factors for semi-elliptical cracks with high aspect ratios by using the tetrahedral finite element (fully automated parametric study)', Engineering Fracture Mechanics. Elsevier Ltd, 158, pp. 144–166. doi: 10.1016/j.engfracmech.2016.02.049.

[21] Zareei, A. and Nabavi, S. M. (2016) 'Calculation of stress intensity factors for circumferential semi-elliptical cracks with high aspect ratio in pipes', International Journal of Pressure Vessels and Piping. Elsevier Ltd, 146, pp. 32–38. doi: 10.1016/j.ijpvp.2016.05.008.

[22] Shariati, M., Mohammadi, E. and Masoudi Nejad, R. (2017) 'Effect of a new specimen size on fatigue crack growth behavior in thick-walled pressure vessels', International Journal of Pressure Vessels and Piping. Elsevier Ltd, 150, pp. 1–10. doi: 10.1016/j.ijpvp.2016.12.009.

[23] Aliha, M. R. M. and Gharehbaghi, H. (2017) 'The effect of combined mechanical load/welding residual stress on mixed mode fracture parameters of a thin aluminum cracked cylinder', Engineering Fracture Mechanics. Elsevier Ltd, 180, pp. 213–228. doi: 10.1016/j.engfracmech.2017.05.003.

[24] Alizadeh Kaklar, J. and Saeidi Googarchin, H. (2018) 'Approximate stress intensity factors for a semi-circular crack in an arbitrary structure under arbitrary mode I loading', Theoretical and Applied Fracture Mechanics. Elsevier Ltd, 94, pp. 71–83. doi: 10.1016/j.tafmec.2018.01.007.

[25] Ramezani, M. K. et al. (2018) 'Empirical solutions for stress intensity factors of a surface crack in a solid cylinder under pure torsion', Engineering Fracture Mechanics. Elsevier, 193(June 2017), pp. 122–136. doi: 10.1016/j.engfracmech.2018.02.015.

[26] Shlyannikov, V. N., Yarullin, R. R. and Ishtyryakov, I. S. (2018) 'Effect of temperature on the growth of fatigue surface cracks in aluminum alloys', Theoretical and Applied Fracture Mechanics. Elsevier Ltd, 96, pp. 758–767. doi: 10.1016/j.tafmec.2017.11.003.

[27] Kheirikhah, M. M. and Khalili, S. M. R. (2011) 'Fracture analysis of semielliptical cracks at the interface of two functionally gradient materials using three-dimensional finite-element method', Proceedings of the Institution of Mechanical Engineers, Part L: Journal of Materials: Design and Applications, 225(2), pp. 49–59. doi: 10.1177/1464420710397640.

[28] Nami, M. R. and Eskandari, H. (2012) 'Three-dimensional investigations of stress intensity factors in a thermo-mechanically loaded cracked FGM hollow cylinder', International Journal of Pressure Vessels and Piping. Elsevier Ltd, 89, pp. 222–229. doi: 10.1016/j.ijpvp.2011.11.004.

[29] Seifi, R. (2015) 'Stress intensity factors for internal surface cracks in autofrettaged functionally graded thick cylinders using weight function method', Theoretical and Applied Fracture Mechanics. Elsevier Ltd, 75, pp. 113–123. doi: 10.1016/j.tafmec.2014.11.004.

[30] Farahpour, P., Babaghasabha, V. and Khadem, M. (2015) 'Stress intensity factor calculation for semi-elliptical cracks on functionally graded material coated cylinders', Structural Engineering and Mechanics, 55(6), pp. 1087–1097. doi: 10.12989/sem.2015.55.6.1087.

[31] Chen, J. and Pan, H. (2013) 'Stress intensity factor of semi-elliptical surface crack in a cylinder with hoop wrapped composite layer', International Journal of Pressure Vessels and Piping. Elsevier Ltd, 110, pp. 77–81. doi: 10.1016/j.ijpvp.2013.04.026.

[32] Eskandari, H. (2016) 'Stress intensity factor of semi-elliptical surface crack in a thermo-mechanically loaded cylinder with hoop wrapped FGM layer', Journal of the Brazilian Society of Mechanical Sciences and Engineering, 38(8), pp. 2563–2570. doi: 10.1007/s40430-016-0495-9.

[33] Eskandari, H. (2018) 'Three-dimensional investigation of cracked tubes coated with functionally graded material under shock loading', Journal of the Brazilian Society of Mechanical Sciences and Engineering. Springer Berlin Heidelberg, 40(9), pp. 1–9. doi: 10.1007/s40430-018-1352-9.

[34] Murtaza, U.T., Heydar, M. J. (2017) 'Stress intensity factors of corner cracks at set-in nozzle–cylinder intersection of a PWR reactor pressure vessel', J Brazilian Soc Mech Sci Eng.,39(2): 601–11. https://doi.org/10.1007/s40430-016-0522-x..

[35] Wang, L. et al. (2017) 'Finite-Element Analysis of Crack Arrest Properties of Fiber Reinforced Composites Application in Semi-Elliptical Cracked Pipelines', Applied Composite Materials. Applied Composite Materials. doi: 10.1007/s10443-017-9621-9.

[36] Rekbi, F. M. L., Hecini, M. and Khechai, A. (2018) 'Experimental and numerical analysis of mode-I interlaminar fracture of composite pipes', Journal of the Brazilian Society of Mechanical Sciences and Engineering, 40(10), p. 502. doi: 10.1007/s40430-018-1423-y.

[37] Ugural, A. (2009) Stresses in beams, plates, and shells. CRC press; 2009. https://doi.org/10.1201/b17516.

[38] Barsoum, R. S. (1976) 'On the use of isoparametric finite elements in linear fracture mechanics', International Journal for Numerical Methods in Engineering, 10(1), pp. 25–37. doi: 10.1002/nme.1620100103.